Report

Current Biology

The Early Ediacaran *Caveasphaera* Foreshadows the Evolutionary Origin of Animal-like Embryology

Graphical Abstract

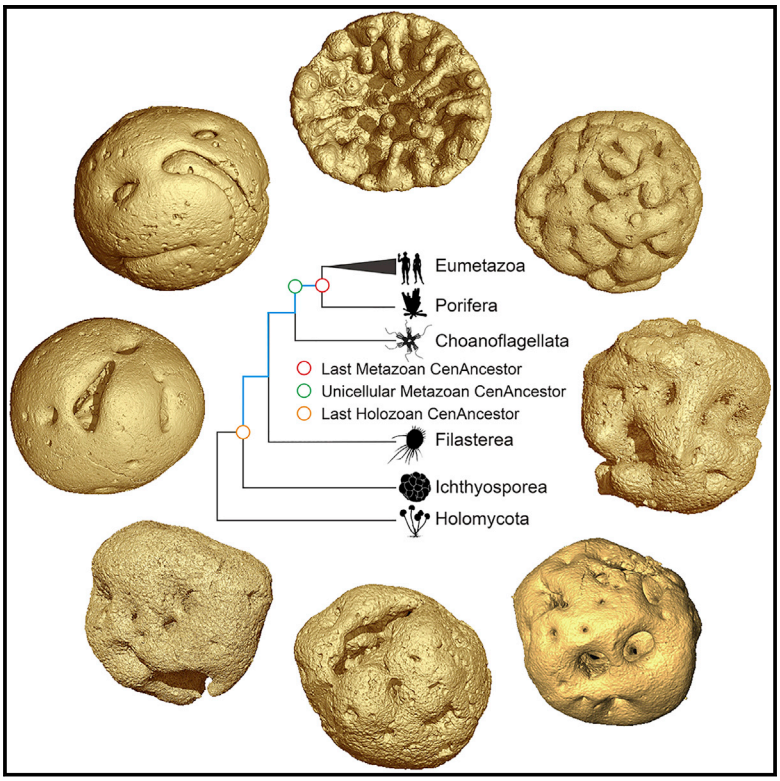

Highlights

- *Caveasphaera* is an enigmatic component of the 609-Ma Weng'an Biota of South China
- Yin et al. use X-ray tomography to characterize cellular structure and development
- Gastrulation-like cell division, ingression, detachment, and polar aggregation occur
- A holozoan affinity suggests the early evolution of metazoan-like development

Authors

Zongjun Yin, Kelly Vargas, John Cunningham, Stefan Bengtson, Maoyan Zhu, Federica Marone, Philip Donoghue

Correspondence

zjyin@nigpas.ac.cn (Z.Y.), phil.donoghue@bristol.ac.uk (P.D.)

In Brief

Yin et al. use X-ray microtomography to show that the 609-Ma-old *Caveasphaera* develops within an envelope by cell division, ingression, detachment, and polar aggregation in a manner analogous to gastrulation. Together with evidence of functional cell adhesion and development within an envelope, this is suggestive of a holozoan affinity.

Yin et al., 2019, Current Biology *29*, 1–8
December 16, 2019 © 2019 Elsevier Ltd.
https://doi.org/10.1016/j.cub.2019.10.057

CellPress

Please cite this article in press as: Yin et al., The Early Ediacaran *Caveasphaera* Foreshadows the Evolutionary Origin of Animal-like Embryology, Current Biology (2019), https://doi.org/10.1016/j.cub.2019.10.057

Current Biology
Report

CellPress

The Early Ediacaran *Caveasphaera* Foreshadows the Evolutionary Origin of Animal-like Embryology

Zongjun Yin,[1,6,*] Kelly Vargas,[2,6] John Cunningham,[2] Stefan Bengtson,[3] Maoyan Zhu,[1,5] Federica Marone,[4] and Philip Donoghue[2,7,*]

[1]State Key Laboratory of Palaeobiology and Stratigraphy, Nanjing Institute of Geology and Paleontology & Center for Excellence in Life and Paleoenvironment, Chinese Academy of Sciences, Nanjing 210008, China
[2]School of Earth Sciences, University of Bristol, Life Sciences Building, Tyndall Avenue, Bristol BS8 1TQ, UK
[3]Department of Palaeobiology, Swedish Museum of Natural History, Box 50007, 104 05 Stockholm SE, Sweden
[4]Swiss Light Source, Paul Scherrer Institute, 5232 Villigen, Switzerland
[5]College of Earth and Planetary Sciences, University of Chinese Academy of Sciences, Beijing 100049, China
[6]These authors contributed equally
[7]Lead Contact
*Correspondence: zjyin@nigpas.ac.cn (Z.Y.), phil.donoghue@bristol.ac.uk (P.D.)
https://doi.org/10.1016/j.cub.2019.10.057

SUMMARY

The Ediacaran Weng'an Biota (Doushantuo Formation, 609 Ma old) is a rich microfossil assemblage that preserves biological structure to a subcellular level of fidelity and encompasses a range of developmental stages [1]. However, the animal embryo interpretation of the main components of the biota has been the subject of controversy [2, 3]. Here, we describe the development of *Caveasphaera*, which varies in morphology from lensoid to a hollow spheroidal cage [4] to a solid spheroid [5] but has largely evaded description and interpretation. *Caveasphaera* is demonstrably cellular and develops within an envelope by cell division and migration, first defining the spheroidal perimeter via anastomosing cell masses that thicken and ingress as strands of cells that detach and subsequently aggregate in a polar region. Concomitantly, the overall diameter increases as does the volume of the cell mass, but after an initial phase of reductive palinotomy, the volume of individual cells remains the same through development. The process of cell ingression, detachment, and polar aggregation is analogous to gastrulation; together with evidence of functional cell adhesion and development within an envelope, this is suggestive of a holozoan affinity. Parental investment in the embryonic development of *Caveasphaera* and co-occurring *Tianzhushania* and *Spiralicellula*, as well as delayed onset of later development, may reflect an adaptation to the heterogeneous nature of the early Ediacaran nearshore marine environments in which early animals evolved.

RESULTS

The Weng'an biota provides a unique insight into multicellular life in the early Ediacaran period, during which molecular clocks estimate the fundamental animal lineages to have diverged [6]. Indeed, there are numerous claims of animal remains from the biota, including miniature adult eumetazoans [7] and bilaterians [8], and embryonic animals [2, 9–12], but all remain contentious [3, 13–18]. However, there is a broader diversity of fossil remains from this deposit that have been the subject of little attention, some of which may have a greater claim on animal affinity. These fossils include *Caveasphaera costata* (Figure 1), which has been described as a spherical hollow cage (Figures 1A–1C) [4] to a more solid sphere (Figure 1D) [5] of unknown nature and affinity, though superficial comparison has been drawn to embryos of an octocoral [4]. Analysis of the structure and development of *Caveasphaera* is challenging because of its small size and complex morphology. We employed synchrotron radiation X-ray tomographic microscopy (srXTM) [19] and high-resolution X-ray microtomography [20] to analyze 233 specimens of *Caveasphaera* that encompass its morphological and size range, based on a rich fossil assemblage from "54" and Datang quarries in the Baiyan-Gaoping Anticline of Weng'an County, Guizhou Province, South China [21].

The cage-like and solid morphs have been interpreted to reflect intraspecific variation [5] but instead represent members of a more continuous spectrum of morphological variation (Figures 1 and 2). *Caveasphaera* is a rare component of the Weng'an Biota, distinguished by its comparatively small cells, organized into a distinctive hollow spheroidal cage delimited by branching strands of cells and radial cell strands (Figures 1 and 2). Earlier stages are lensoidal but can be associated reliably because they are composed of cells of similar phenotype and exhibit the characteristic arrangement of polarized and branching cell masses (Figures 1A, 2A, and 2B). The latest stages identified are increasingly solid but can be associated based on their transitional continuum with earlier hollow stages (Figures 2C–2R). Although there is some taphonomic variation within the assemblage, 70 specimens are preserved in high fidelity (Figures 1 and 2), demonstrating a cellular composition in which polygonal cells are closely packed with Y-shaped interfaces (Figures 1E, 1F, and 2U–2Z). Quantitative computed tomography of the srXTM data demonstrates little variation in the volume of component cells within any one specimen and across development (Figure 3A)—with the exception of the lensoidal stages that

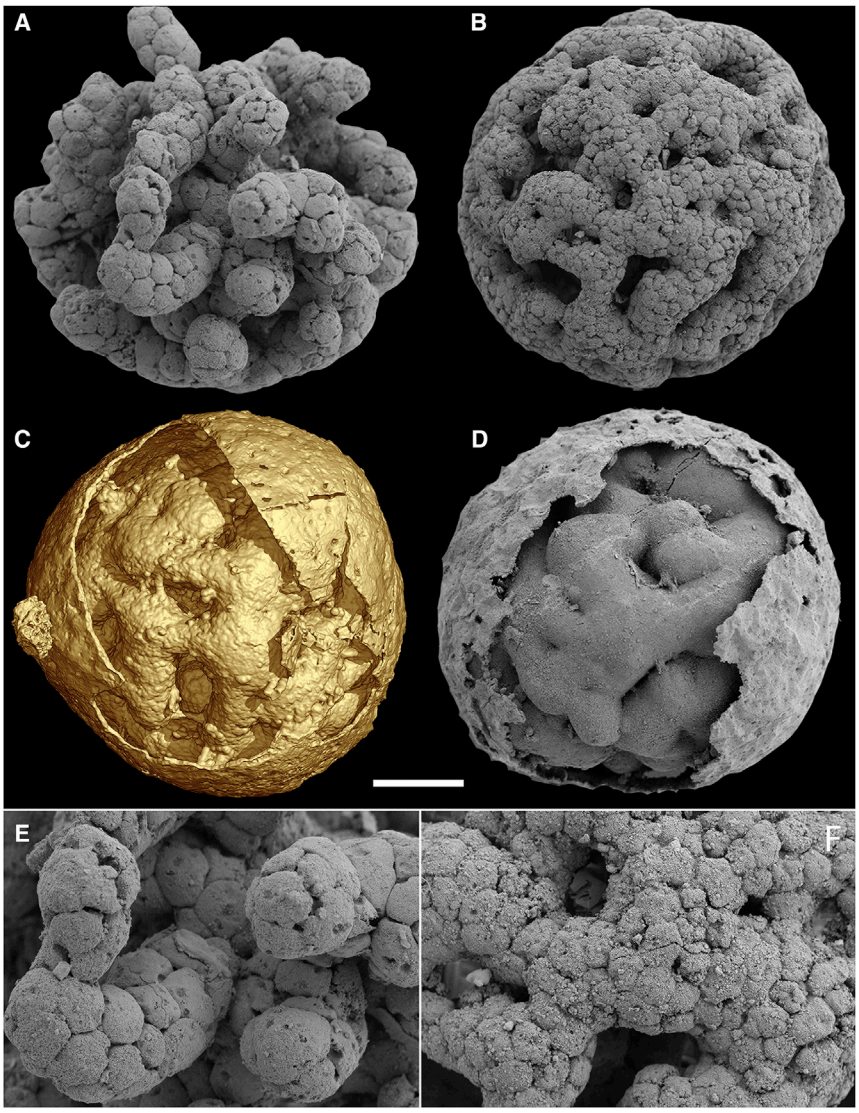

Figure 1. General Biology of *Caveasphaera*

(A and B) Naked early and later stage specimens with cellular structure.

(C and D) Specimens with envelopes.

(E and F) Close-up views of (A) and (B), respectively, showing detail of cellular structures.

See also Figure S1. Scale bars, 85 μm for (A) (NIGP171727); 95 μm for (B) (NIGP171728); 130 μm for (C) (NIGP171725); 90 μm for (D) (NIGP171729); 40 μm for (E); and 38 μm for (F). Tomographic models appear gold and scanning electron micrographs appear in greyscale.

have larger and fewer cells (Figures 1A and 1E). Across the range of specimens, there is an almost 2-fold (373–735 μm) increase in diameter and a more than 8-fold increase in the sum volume of cells (0.0171–0.2 mm^3; Figure 3B; the raw data for Figure 3 is available in Data S1).

Almost all of the specimens of *Caveasphaera* in our collection lack an enclosing envelope, and for most of the specimens with an envelope, it is difficult to exclude the possibility that the association is taphonomic (e.g., Figures S1K and S1L). The paucity of specimens preserving an envelope is a reflection of the practical challenge of attributing specimens to *Caveasphaera* when their morphology is obscured by an envelope. Nevertheless, a small number of specimens representative of early and late stages of development are preserved in association with incomplete envelopes (Figures 1C, 1D, and S1A–S1J), and the broken openings into these are too small to support a post mortem taphonomic association. The envelopes range in diameter from 504 to 806 μm and, when completely preserved, have two layers, the outermost of which has an approximately polygonal verrucose ornament reminiscent of the "Megasphaera" taphomorph of *Tianzhushania* (Figures S1C, S1D, S1G, and S1H); this is more often lost taphonomically, revealing the smooth and featureless inner layer (Figures 1C, 1D, S1E, S1F, and S1I), as is common with other embryo-like fossils from the Weng'an Biota [23]. The thickness of the inner envelope varies with the degree of void-filling diagenetic mineralization (compare Figures S1E, S1F, and S1I versus Figures S1J–S1L).

The specimens with among the lowest aggregate volume of cells have a lensoidal morphology with one smooth convex surface and another from which cellular protuberances emerge (Figures 1A, 2A, and 2B). The smallest hollow spheroidal specimens are composed of an interconnected network of anastomosing branches that show evidence of bifurcation, coalescence, and radial ingression (Figures 1B, 2C, 2D, 2K, and 2L). The branching meshwork of cells defining the perimeter increases in size across specimens of progressive development (Figures 1A, 1B, and 2A–2C versus Figures 2E, 2F, 2M, and 2N) and shows branching within this plane as well as radially toward the center, where it occupies the volume defined by the perimeter, as evidenced by laterally and internally protruding "tails" (Figures 1A, 2C–2E, 2K–2M, 2O, 2U, 2W, 4C, 4D, S2B, and S2F). Consequently, the spheroidal perimeter is more continuous, with fewer and smaller openings to the interior (Figures 2G–2J); the depth of the perimeter cell layer also increases (Figures 2K and 2L versus Figures 2N–2Q). However, although the outer surface of the cell mass is smooth and convex, the inner surface is generally concave and irregular (Figures 2M, 2O, and 2P), as a consequence of inwardly extending strands of cells (Figures 2U and 2W). In part, this appears to reflect ingression of cells and cell clusters from the inner surface of the circumferential cell mass. This appears to have occurred individually, as evidenced by the development of constrictions in the radial cell strands to define barely attached cell clusters (Figures 2L, 2M, 2T, and 2U), as well as isolated cell clusters that occur only within the lumen (Figures 4A–4D, 4I, 4J, and S2A–S2L). Although taphonomy experiments have shown that cells within cleavage

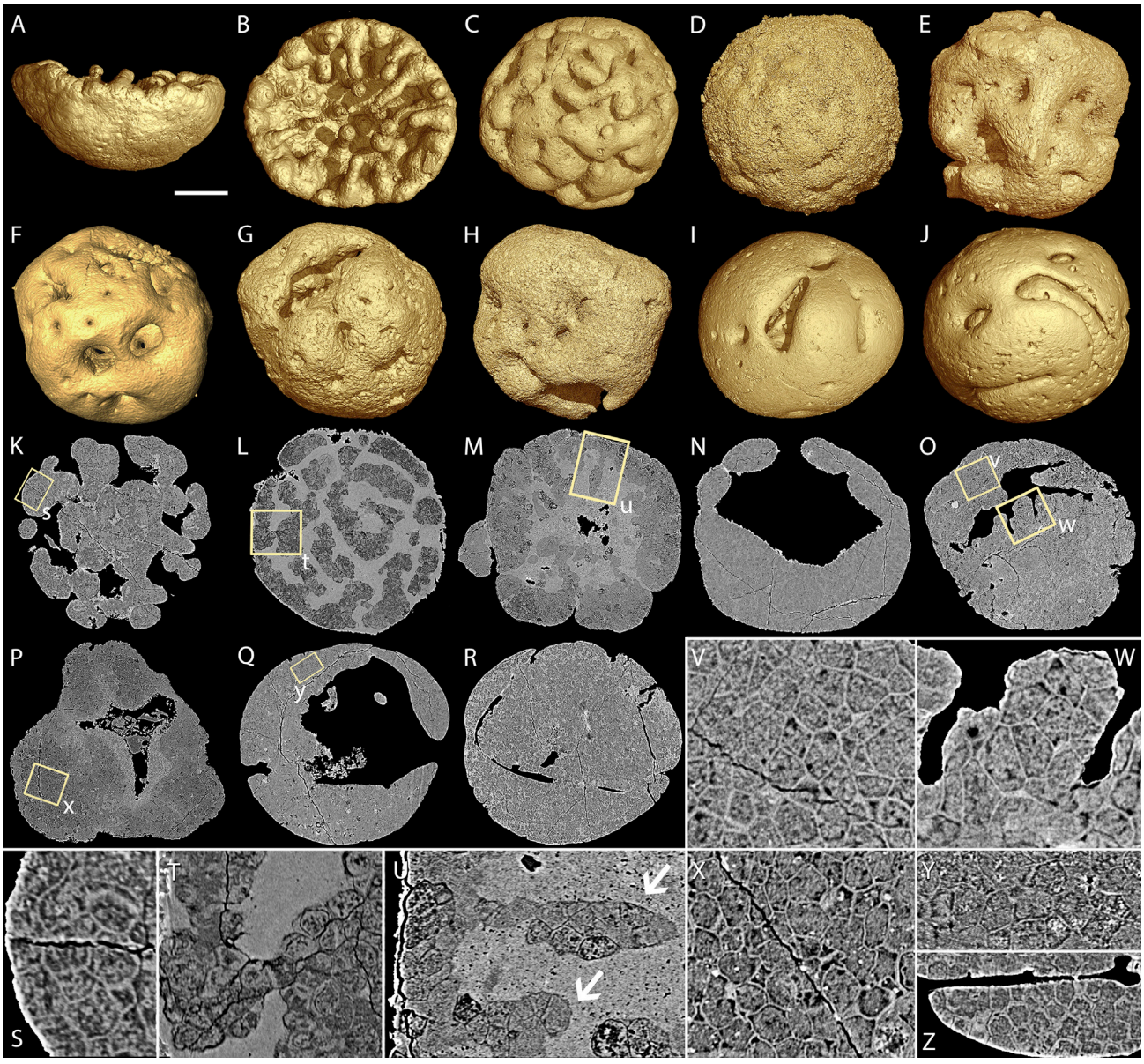

Figure 2. Different Developmental Stages of *Caveasphaera*

(A–J) Morphology of naked *Caveasphaera* exhibiting successive stages of development. (A) and (B) represent lateral and polar views of the same earliest stage. (K–R) Virtual slices of (C)–(J), respectively, showing internal structures.

(S–Z) Close-up views of (K)–(M), (O), (P), and (R), respectively, showing cellular structure. The arrows in (U) and (W) indicate inwardly extending strands of cells. See also Figure S2. Scale bars, 200 μm for (A) and (B) (NIGP171515); 120 μm for (C) and (K) (NIGP171623); 130 μm for (D), (L), (N), and (Q) (NIGP171667); 160 μm for (E) (NIGP171557); 155 μm for (F) (NIGP171610); 118 μm for (G) (NIGP171633); 176 μm for (H) (NIGP171581); 145 μm for (I) (NIGP171583); 185 μm for (J) (NIGP171502); 150 μm for (M); 114 μm for (O); 154 μm for (P); 177 μm for (R); 43 μm for (S); 27 μm for (T); 33 μm for (U); 21 μm for (V) and (W); 26 μm for (X); 20 μm for (Y); and 27 μm for (Z).

and gastrula embryos can lose adhesion post mortem [24], cell ingression seems to have occurred *in vivo* in *Caveasphaera* because there is direct evidence of cell masses coalescing (Figures 2L and 2T), which occurs in parallel with polar thickening of the cortex of cells, resulting in a thick-based, approximately cup-shaped body that reaches up around 80%–90% of the spheroid volume (Figures 2F, 2I, 2N, and 2Q). Our largest specimen is an almost solid spheroid of cells preserving evidence of the infilling of the central void with cells (Figures 2J, 2R, and 2Z). There is no evidence of the cell phenotype differentiation seen in other multicellular organisms in the Weng'an Biota [3, 25], nor do we have specimens representative of what must be the very earliest stages of development, composed of few cells.

Among our collection of specimens, the aggregate volume of cells comprising specimens increases broadly and continuously with size (Figure 3B). Aside from the lensoidal stage (Figures 1A,

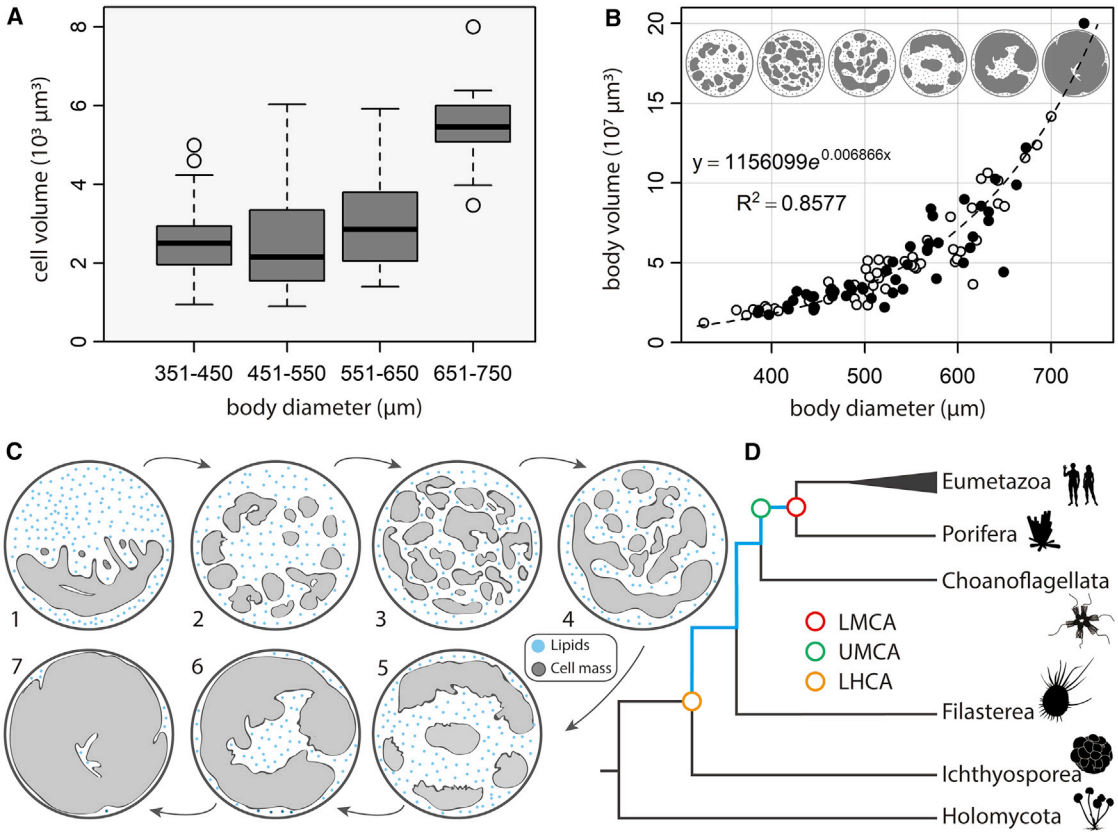

Figure 3. Developmental Biology and Phylogenetic Affinity of *Caveasphaera*

(A) Box plot of body diameter (diameter of naked spheroidal body of cell mass) and individual cell volume, showing little variation of cell volume/size across different specimens. Individual volume of cells (137 cells in total) was measured from 27 well-preserved specimens with clear cell boundaries (refer to Data S1 for raw data).

(B) Non-linear relationship between body diameter and body volume (that is, the sum of cell volumes). The body diameter and volume were measured based on 100 unbroken specimens' segmented volume data (refer to Data S1 for raw data). The filled and unfilled circles represent specimens with and without cellular structures, respectively. The row of cartoons is stylized representations of the cross-sectional morphology of *Caveasphaera* at different developmental stages, reflecting the broad correlation between the size and morphology of these developmental stages.

(C) *Caveasphaera* develops from small, hollow cage stages to larger solid stages within a two-layered envelope.

(D) A simplified phylogenetic tree of Holozoa, with Holomycota as the outgroup [22]. LHCA, last holozoan common ancestor; LMCA, last metazoan common ancestor; UMCA, unicellular metazoan common ancestor. The potential placements for *Caveasphaera* in the holozoan tree are indicated in blue.

2A, and 2B), the average volume of individual cells shows little variation between those in the center of the body versus the perimeter (mean and SD of 2,881 μm^3 and 1,318 μm^3 versus 3,197 μm^3 and 1,288 μm^3, respectively). There is no explicit correlation between specimen and cell size variables, and the volume of individual cells remains in a similar range among specimens from different size classes (Figure 3A). These facts require that the increase in the aggregate volume of cells among specimens is achieved largely through cell addition rather than through increase in the volume of individual cells (Figure 3B). Additional cells must have emerged through cell division and growth; as this is not observed, it must have occurred at the time of cell division. Some of this variance in aggregate cell volume can be accounted for as a taphonomic artifact or developmental variation because many of the specimens we studied preserve cell aggregates that are isolated from the larger cell mass, preserved *in situ* within the central void as a consequence of geological mineralization (Figures 4A–4D and S2; their topology requires that they were held in place by a non-cellular matrix *in vivo*; this non-cellular matrix has been preserved in some specimens, for example, Figures 4E–4H, 4K, 4L, and S3). The isolated cell clusters occur across the size range of specimens and range in number from 1 to 26, with most specimens preserving fewer than 10. Hence, it is likely that the aggregate volume of cells in many of the lower-density cage-like specimens is reduced as a consequence of the loss of isolated cell clusters post mortem. Nevertheless, these isolated cell clusters evidence a process by which the hollow stages develop into their denser, larger counterparts.

The presence of an outer envelope is potentially difficult to rationalize because it requires that the development of *Caveasphaera* (Figure 3C), with a greater than 8-fold increase in volume across specimens in our collection (Figure 3B), proceeded without an external source of nutrients. This contrasts with the

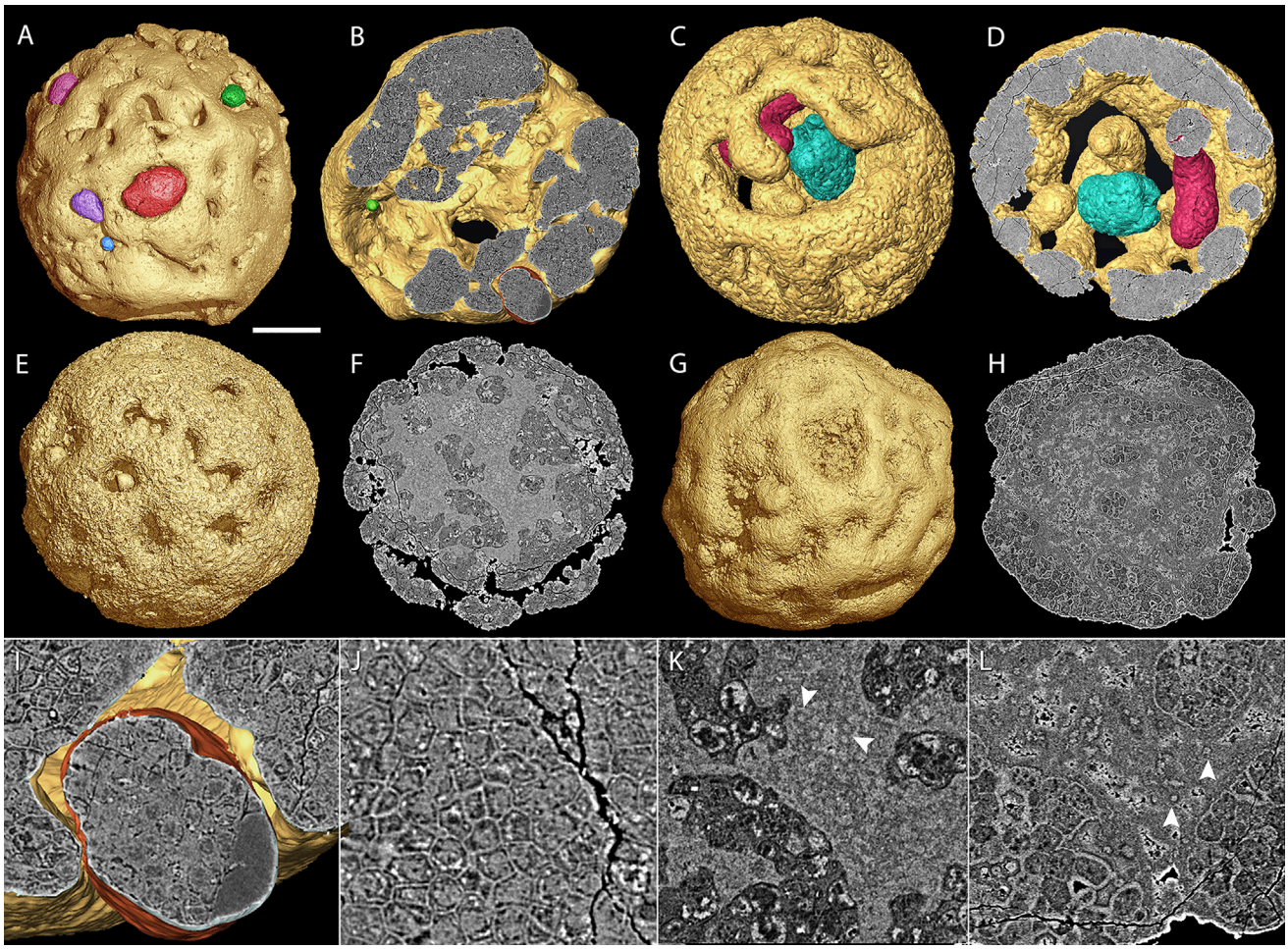

Figure 4. Specimens with Isolated Cell Clusters and Possible Lipid Droplets

(A and C) Surface renderings; the cell clusters were indicated by red, cyan, green, pink, purple, and blue.

(B and D) Virtual three-dimensional sections of (A) and (C), respectively.

(E and G) Surface renderings of (F) and (H).

(F and H) Virtual slices of (E) and (G), respectively, showing preserved intercellular matrix.

(I and J) Close-up views of (B), showing cellular structures of isolated cell cluster and cell mass.

(K and L) Close-up views of (F) and (H), respectively, showing lipid-like vesicles (arrowheads).

See also Figure S3. Scale bars, 150 μm for (A) (NIGP171538); 140 μm for (B); 110 μm for (C) and (D) (NIGP171455); 85 μm for (E) and (F) (NIGP171651); 120 μm for (G) and (H) (NIGP171585); 35 μm for (I); 27 μm for (J); 30 μm for (K); and 38 μm for (L).

pattern of development exhibited by *Tianzhushania* and *Spiralicellula* from the same deposit, which exhibit a more approximately constant volume across a pattern of binary reductive palintomy [3, 26]. This could be rationalized in *Caveasphaera* if the true pattern of development is the reverse of that described in Figure 3C, where the larger, denser specimens represent the earliest stages and development proceeds through the loss of cells, perhaps as propagules or gametes, detaching first from the interior as individual cells and clusters, with the overall cell mass reshaping and resizing through this process. However, the enclosing envelope makes this interpretation unlikely, if not impossible, because the expectation of hundreds of loose cells entrained within the envelope but outside the lumen is not met. The difference in cell size between the lensoidal and spheroidal morphs also strongly suggests that they represent early and later stages, respectively. *Tianzhushania* and *Spiralicellula* both preserve evidence of intracellular lipids in specimens representative of the first few rounds of palintomy [17], but these cells are orders of magnitude larger than the cells of *Caveasphaera*; comparably sized cells representative of later stages of palintomy show no such evidence. Nevertheless, two specimens of *Caveasphaera* preserve an extracellular matrix containing spheroidal structures that are smaller than the polygonal cells (Figures 4E–4H, 4K, 4L, and S3). These exhibit comparable preservation to the structures interpreted as intracellular lipid droplets in *Tianzhushania* and *Spiralicellula* [17, 26], suggesting that these developmental stages of *Caveasphaera* may have been invested in extracellular lipids that sustained growth and development within the closed, enveloped environment.

DISCUSSION

The multicelled organization of *Caveasphaera* invites comparison to prokaryotes and eukaryotes with multicellular stages in their life cycles. The branching arrangement of cell masses seen in the cyanobacterium *Microcystis* [27, 28] are particularly reminiscent of *Caveasphaera*, but *Microcystis* does not comprise spheroids in this planktonic conformation [29]. Like other prokaryote multicellular colonies, *Microcystis* lacks the enclosing envelope of *Caveasphaera*; the cells are physically separate, bound together (through aggregation or vegetative association) [30] by mucilage [31], and so the cells do not exhibit the Y-shaped intercell junctions seen in *Caveasphaera*, which are indicative of cell adhesion. Bacterial cysts form from thickening of the cell wall but are unicellular. Bacterial endospores are usually singular, forming within the mother cell wall; exceptionally, up to nine endospores can form per cell [32], but even in such circumstances, the endospores do not exhibit the Y-shaped intercell conformation exhibited by *Caveasphaera*. Indeed, Y-shaped intercell junctions are commonly interpreted to reflect flexible cell membranes and functional cell adhesion indicative of tissue-grade multicellularity and, specifically, an animal affinity [1, 2, 33, 34]. However, diverse eukaryotes exhibit multicellular stages in their life cycles [35], many of which have cells arranged with Y-shaped intercell junctions [21]. Because multicellularity has evolved many times among extant eukaryotes, *Caveasphaera* might belong to any one of these living or (likely many more) extinct lineages of multicellular eukaryotes.

For example, apicomplexans, such as *Perkinsus*, also possess multicellular hypnospores and zoospores encapsulated within a cyst [36, 37], as do the chlorophytes *Ulothrix* and *Chlorococcum*, whereas chlorophytes, such as *Spirogyra*, and dinophyceaecean dinoflagellates provide encysted hypnozygotes of comparable grade [38]. Rhodophytes, such as *Ptilothamnion*, also produce polysporangiate spore masses that arise from repeated rounds of division beyond those that normally produce tetraspores [39]. Animals, plants, as well as red, brown, and green algae all exhibit multicellular embryonic development [35]. The embryos of phaeophytes differentiate quickly, with rhizoid development apparent from before the first round of palintomy [40]; carpospore development in rhodophytes goes through more rounds of development, but sporophyte morphogenesis is apparent within four or five rounds of palintomy [41, 42]. In both phaeophytes and rhodophytes, the embryos are initially naked, only subsequently developing an irregular mucilaginous sheath [43, 44]. Volvocine algae exhibit cellular differentiation and recurrent rounds of palintomy, a process of inversion that resembles patterns of gastrulation in some animals [45], and some volvocines also produce complex ornamented cysts [46]. However, the coordinated arrangement of cells in the multicellular zygotes of volvocines is achieved through incomplete cell division that appears ancestral [47].

None of these examples bear close comparison to *Caveasphaera* in that either their component cells are relatively small in number and uncoordinated (hypnospores, hypnozygotes, and polysporangia), they lack a resting cyst and undergo rapid morphogenesis with only a single cell or a few tens of cells (phaeophyte embryos and rhodophyte carpospores), or they achieve cell coordination through incomplete cell division (volvocines). Much greater coordinated arrangement is exhibited by holozoans, such as the ichthyosporeans *Creolimax*, *Pirum*, and *Sphaeroforma* which, along with filastereans, possess a spheroidal multicellular stage composed of tens to hundreds of cells with Y-shaped intercell junctions facilitated by functional cell adhesion [22]. Ichthyosporeans like *Sphaeroforma* develop initially as a multinucleate coenocyte [48] before undergoing cytokinesis to form a blastocoel-like structure with an epithelium-like perimeter of cells enclosed within an envelope [49–51]; the cells ultimately disaggregate and are released to the environment [51]. Thus, among eukaryotes that exhibit a multicellular embryo, spore, or sporangial stage, the number of cells and patterns of cell adhesion and rearrangement inferred in the development of *Caveasphaera* bear close comparison only to the multicellular stages of non-metazoan holozoans and animal embryos. The arrangement of cells, defining an incomplete perimeter of the overall spheroid, is also seen in animal embryos [52, 53]. The overall arrangement of cells defining a perimeter around a central cavity is reminiscent of ichthyosporeans and the blastocoels of animal embryos. The inferred pattern of cell ingression, detachment, and subsequent polar aggregation is comparable to gastrulation. Indeed, the pattern of branching cell masses is similar to the process of elongation associated with the developing gastrulae and planulae of cnidarians like *Hydractinia* [54], perhaps reflecting a similar process of embryonic development. Because the many alternative non-holozoan instances of convergently evolved aggregative or embryonic multicellularity are much more similar to one another than the more complex development of *Caveasphaera*, its similarities to holozoan and metazoan embryonic development are less likely to represent an extinct independent instantiation of embryonic multicellularity.

The developmental biology of *Caveasphaera* (Figure 3C) is more similar to the embryos of crown-metazoans than it is to outgroups, including the choanoflagellates, filastereans, and ichthyosporeans (non-metazoan holozoans; Figure 3D), all of which have a coordinated multicellular stage in what are otherwise unicellular life histories [22]. In large part, this is facilitated by the shared components of what has been perceived to be a metazoan developmental toolkit of transcription factors, cell adhesion, and cell-signaling molecules [55], elements of which have been lost in filastereans and choanoflagellates [22, 55], reflecting lost ancestral complexity that may belie the distinctive complexity of metazoan body plans and their development, with respect to their holozoan [22] or opisthokont [56] ancestry. For this reason, we cannot discriminate the possibility that *Caveasphaera* was a close holozoan relative of metazoans from the possibility that it represents a stem- or crown-metazoan (Figure 3D). Therefore, we hold back on concluding that *Caveasphaera* evidences the origin of animals and their embryology, but it clearly indicates that processes similar to gastrulation, which is a shared primitive feature of metazoans [57], were present already by the early Ediacaran. In this regard, it is interesting that the development of *Caveasphaera* was invested in parental resources, like the large and lipid-rich *Tianzhushania* and *Spiralicellula*. This, together with the apparently delayed onset of later development—extending beyond thousands of cells—presumably reflects adaptation to the temporally and spatially heterogeneous nature of environmental conditions that prevailed in early Ediacaran nearshore marine environments [58]. In this sense, the

attendant adverse geochemical environments do not appear to have constrained these formative steps in the evolutionary origins of animal complexity.

STAR★METHODS

Detailed methods are provided in the online version of this paper and include the following:

- KEY RESOURCES TABLE
- LEAD CONTACT AND MATERIALS AVAILABILTY
- EXPERIMENTAL MODEL AND SUBJECT DETAILS
- METHOD DETAILS
  - Specimen recovery
  - Scanning Electron Microscopy
  - X-Ray and Computed Tomography
- QUANTIFICATION AND STATISTICAL ANALYSIS
- DATA AND CODE AVAILABILITY

SUPPLEMENTAL INFORMATION

Supplemental Information can be found online at https://doi.org/10.1016/j.cub.2019.10.057.

ACKNOWLEDGMENTS

This study was supported by Strategic Priority Research Program (B) of the Chinese Academy of Sciences (CAS) (XDB 26000000 and 18000000 to Z.Y. and M.Z.), Newton Advanced Fellowship (to Z.Y. and P.D.), the Natural Environment Research Council (NE/P013678/1 to P.D. and Z.Y.), National Natural Science Foundation of China (41672013 to Z.Y. and P.D.), and the Youth Innovation Promotion Association of the CAS (2017360 to Z.Y.). We also received funding from the European Union's Horizon 2020 research and innovation programme under grant agreement no. 730872, project CALIPSOplus. Finally, we acknowledge the Paul Scherrer Institute, Villigen, Switzerland, for provision of synchrotron radiation beamtime at the TOMCAT beamline of the Swiss Light Source.

AUTHOR CONTRIBUTIONS

P.D. and Z.Y. designed the project and managed it to completion. S.B., J.C., P.D., F.M., K.V., and Z.Y. collected the data, and K.V. led the analysis of the data to which all authors contributed. P.D., K.V., and Z.Y. led both the interpretation of the results and the writing, to which all authors contributed.

DECLARATION OF INTERESTS

The authors declare no competing interests.

Received: May 24, 2019
Revised: August 21, 2019
Accepted: October 29, 2019
Published: November 27, 2019

REFERENCES

1. Xiao, S., Muscente, A.D., Chen, L., Zhou, C., Schiffbauer, J.D., Wood, A.D., Polys, N.F., and Yuan, X. (2014). The Weng'an biota and the Ediacaran radiation of multicellular eukaryotes. Natl. Sci. Rev. *1*, 498–520.
2. Chen, L., Xiao, S., Pang, K., Zhou, C., and Yuan, X. (2014). Cell differentiation and germ-soma separation in Ediacaran animal embryo-like fossils. Nature *516*, 238–241.
3. Huldtgren, T., Cunningham, J.A., Yin, C., Stampanoni, M., Marone, F., Donoghue, P.C.J., and Bengtson, S. (2011). Fossilized nuclei and germination structures identify Ediacaran "animal embryos" as encysting protists. Science *334*, 1696–1699.
4. Xiao, S., and Knoll, A.H. (2000). Phosphatized animal embryos from the Neoproterozoic Doushantou Formation at Weng'an, Guizhou, South China. J. Paleontol. *74*, 767–788.
5. Xiao, S., Zhou, C., Liu, P., Wang, D., and Yuan, X. (2014). Phosphatized acanthomorphic acritarchs and related microfossils from the Ediacaran Doushantuo Formation at Weng'an (South China) and their implications for biostratigraphic correlation. J. Paleontol. *88*, 1–67.
6. dos Reis, M., Thawornwattana, Y., Angelis, K., Telford, M.J., Donoghue, P.C., and Yang, Z. (2015). Uncertainty in the timing of origin of animals and the limits of precision in molecular timescales. Curr. Biol. *25*, 2939–2950.
7. Xiao, S., Yuan, X., and Knoll, A.H. (2000). Eumetazoan fossils in terminal proterozoic phosphorites? Proc. Natl. Acad. Sci. USA *97*, 13684–13689.
8. Chen, J.-Y., Bottjer, D.J., Oliveri, P., Dornbos, S.Q., Gao, F., Ruffins, S., Chi, H., Li, C.W., and Davidson, E.H. (2004). Small bilaterian fossils from 40 to 55 million years before the Cambrian. Science *305*, 218–222.
9. Xiao, S., Zhang, Y., and Knoll, A.H. (1998). Three-dimensional preservation of algae and animal embryos in a Neoproterozoic phosphorite. Nature *391*, 553–558.
10. Chen, J.-Y., Bottjer, D.J., Li, G., Hadfield, M.G., Gao, F., Cameron, A.R., Zhang, C.-Y., Xian, D.-C., Tafforeau, P., Liao, X., and Yin, Z.J. (2009). Complex embryos displaying bilaterian characters from Precambrian Doushantuo phosphate deposits, Weng'an, Guizhou, China. Proc. Natl. Acad. Sci. USA *106*, 19056–19060.
11. Chen, J.Y., Bottjer, D.J., Davidson, E.H., Dornbos, S.Q., Gao, X., Yang, Y.H., Li, C.W., Li, G., Wang, X.Q., Xian, D.C., et al. (2006). Phosphatized polar lobe-forming embryos from the Precambrian of southwest China. Science *312*, 1644–1646.
12. Chen, J.Y., Oliveri, P., Li, C.-W., Zhou, G.-Q., Gao, F., Hagadorn, J.W., Peterson, K.J., and Davidson, E.H. (2000). Precambrian animal diversity: putative phosphatized embryos from the Doushantuo Formation of China. Proc. Natl. Acad. Sci. USA *97*, 4457–4462.
13. Cunningham, J.A., Thomas, C.-W., Bengtson, S., Kearns, S.L., Xiao, S., Marone, F., Stampanoni, M., and Donoghue, P.C.J. (2012). Distinguishing geology from biology in the Ediacaran Doushantuo biota relaxes constraints on the timing of the origin of bilaterians. Proc. Biol. Sci. *279*, 2369–2376.
14. Bengtson, S., Cunningham, J.A., Yin, C., and Donoghue, P.C.J. (2012). A merciful death for the "earliest bilaterian," *Vernanimalcula*. Evol. Dev. *14*, 421–427.
15. Zhang, X.-G., and Pratt, B.R. (2014). Possible algal origin and life cycle of Ediacaran Doushantuo microfossils with dextral spiral structure. J. Paleontol. *88*, 92–98.
16. Butterfield, N.J. (2011). Paleontology. Terminal developments in Ediacaran embryology. Science *334*, 1655–1656.
17. Hagadorn, J.W., Xiao, S., Donoghue, P.C.J., Bengtson, S., Gostling, N.J., Pawlowska, M., Raff, E.C., Raff, R.A., Turner, F.R., Chongyu, Y., et al. (2006). Cellular and subcellular structure of neoproterozoic animal embryos. Science *314*, 291–294.
18. Cunningham, J.A., Vargas, K., Pengju, L., Belivanova, V., Marone, F., Martínez-Pérez, C., Guizar-Sicairos, M., Holler, M., Bengtson, S., and Donoghue, P.C.J. (2015). Critical appraisal of tubular putative eumetazoans from the Ediacaran Weng'an Doushantuo biota. Proc. Biol. Sci. *282*, 20151169.
19. Donoghue, P.C.J., Bengtson, S., Dong, X.-P., Gostling, N.J., Huldtgren, T., Cunningham, J.A., Yin, C., Yue, Z., Peng, F., and Stampanoni, M. (2006). Synchrotron X-ray tomographic microscopy of fossil embryos. Nature *442*, 680–683.
20. Yin, Z., Zhao, D., Pan, B., Zhao, F., Zeng, H., Li, G., Bottjer, D.J., and Zhu, M. (2018). Early Cambrian animal diapause embryos revealed by X-ray tomography. Geology *46*, 387–390.

21. Cunningham, J.A., Vargas, K., Yin, Z., Bengtson, S., and Donoghue, P.C.J. (2017). The Weng'an Biota (Doushantuo Formation): an Ediacaran window on soft-bodied and multicellular microorganisms. J. Geol. Soc. *174*, 793–802.
22. Sebé-Pedrós, A., Degnan, B.M., and Ruiz-Trillo, I. (2017). The origin of Metazoa: a unicellular perspective. Nat. Rev. Genet. *18*, 498–512.
23. Xiao, S., Zhou, C., and Yuan, X. (2007). Palaeontology: undressing and redressing Ediacaran embryos. Nature *446*, E9–E10, discussion E10–E11.
24. Raff, E.C., Villinski, J.T., Turner, F.R., Donoghue, P.C.J., and Raff, R.A. (2006). Experimental taphonomy shows the feasibility of fossil embryos. Proc. Natl. Acad. Sci. USA *103*, 5846–5851.
25. Xiao, S., Knoll, A.H., Yuan, X., and Pueschel, C.M. (2004). Phosphatized multicellular algae in the Neoproterozoic Doushantuo Formation, China, and the early evolution of florideophyte red algae. Am. J. Bot. *91*, 214–227.
26. Yin, Z., Cunningham, J.A., Vargas, K., Bengtson, S., Zhu, M., and Donoghue, P.C.J. (2017). Nuclei and nucleoli in embryo-like fossils from the Ediacaran Weng'an Biota. Precambrian Res. *301*, 145–151.
27. Sanchis, D., Carrasco, D., and Quesada, A. (2004). The genus *Microcystis* (Microcystaceae/Cyanobacteria) from a Spanish reservoir: A contribution to the definition of morphological variations. Nova Hedwigia *79*, 479–495.
28. Otsuka, S., Suda, S., Li, R., Matsumoto, S., and Watanabe, M.M. (2000). Morphological variability of colonies of *Microcystis* morphospecies in culture. J. Gen. Appl. Microbiol. *46*, 39–50.
29. Šejnohová, L., and Maršálek, B. (2012). Microcystis. In Ecology of Cyanobacteria II. Their Diversity in Space and Time, B.A. Whitton, ed. (Springer), pp. 195–228.
30. Xiao, M., Willis, A., Burford, M.A., and Li, M. (2017). Review: a meta-analysis comparing cell-division and cell-adhesion in Microcystis colony formation. Harmful Algae *67*, 85–91.
31. Liu, L., Huang, Q., and Qin, B. (2018). Characteristics and roles of *Microcystis* extracellular polymeric substances (EPS) in cyanobacterial blooms: a short review. J. Freshwat. Ecol. *33*, 183–193.
32. Hutchison, E.A., Miller, D.A., and Angert, E.R. (2014). Sporulation in bacteria: beyond the standard model. In In The Bacterial Spore: from Molecules to Systems, First Edition, A. Driks, and P. Eichenberger, eds. (American Society for Microbiology), pp. 87–102.
33. Xiao, S. (2002). Mitotic topologies and mechanics of Neoproterozoic algae and animal embryos. Paleobiology *28*, 244–250.
34. Xiao, S., Knoll, A.H., Schiffbauer, J.D., Zhou, C., and Yuan, X. (2012). Comment on "Fossilized nuclei and germination structures identify Ediacaran 'animal embryos' as encysting protists". Science *335*, 1169, author reply 1169.
35. Rensing, S.A. (2016). (Why) does evolution favour embryogenesis? Trends Plant Sci. *21*, 562–573.
36. Choi, K.-S., and Park, K.-I. (2010). Review on the protozoan parasite *Perkinsus olseni* (Lester and Davis 1981) infection in Asian waters. In Coastal Environmental and Ecosystem Issues of the East China Sea, A. Ishimatsu, and H.-J. Lie, eds. (Terrapub and Nagasaki University), pp. 269–281.
37. Azevedo, C., Corral, L., and Cachola, R. (1990). Fine structure of zoosporulation in *Perkinsus atlanticus* (Apicomplexa: Perkinsea). Parasitology *100*, 351–358.
38. Barsanti, L., and Gualtieri, P. (2014). Algae: Anatomy, Biochemistry, and Biotechnology (CRC Press).
39. Krishnamurthy, V. (2001). Reproductive biology of eukaryotic algae. In Reproductive Biology of Plants, B.M. Johri, and P.S. Srivastava, eds. (Springer, Heidelberg), pp. 57–95.
40. Rusig, A.-M., Ouichou, A., Le Guyader, H., and Ducreux, G. (2001). Ontogenesis in the Fucophyceae: case studies and comparison of fucoid zygotes and *Sphacelaria* apical cells. Cryptogam. Algol. *22*, 227–248.
41. Michetti, K.M., Martín, L.A., and Leonardi, P.I. (2013). Carpospore release and sporeling development in *Gracilaria gracilis* (Gracilariales, Rhodophyta) from the southwestern Atlantic coast (Chubut, Argentina). J. Appl. Phycol. *25*, 1917–1924.
42. Wang, G., Jiang, C., Wang, S., Wei, X., and Zhao, F. (2012). Early development of *Grateloupia turuturu* (Halymeniaceae, Rhodophyta). Chin. J. Oceanology Limnol. *30*, 264–268.
43. Brawley, S.H., Wetherbee, R., and Quatrano, R.S. (1976). Fine-structural studies of the gametes and embryo of *Fucus vesiculosus* L. (Phaeophyta). II. The cytoplasm of the egg and young zygote. J. Cell Sci. *20*, 255–271.
44. Tsekos, I. (1983). The ultrastructure of carposporogenesis in *Gigartina teedii* (Roth) Lamour. (*Gigartinales, Rhodophyceae*): Gonimoblast cells and carpospores. Flora *174*, 191–211.
45. Kirk, D.L. (2000). Volvox as a model system for studying the ontogeny and phylogeny of multicellularity and cellular differentiation. J. Plant Growth Regul. *19*, 265–274.
46. Smith, G.M. (1944). A comparative study of the species of *Volvox*. Trans. Am. Microsc. Soc. *63*, 265–310.
47. Arakaki, Y., Kawai-Toyooka, H., Hamamura, Y., Higashiyama, T., Noga, A., Hirono, M., Olson, B.J., and Nozaki, H. (2013). The simplest integrated multicellular organism unveiled. PLoS ONE *8*, e81641.
48. Ondracka, A., Dudin, O., and Ruiz-Trillo, I. (2018). Decoupling of nuclear division cycles and cell size during the coenocytic growth of the ichthyosporean *Sphaeroforma arctica*. Curr. Biol. *28*, 1964–1969.e2.
49. Suga, H., and Ruiz-Trillo, I. (2013). Development of ichthyosporeans sheds light on the origin of metazoan multicellularity. Dev. Biol. *377*, 284–292.
50. Marshall, W.L., and Berbee, M.L. (2011). Facing unknowns: living cultures (*Pirum gemmata* gen. nov., sp. nov., and *Abeoforma whisleri*, gen. nov., sp. nov.) from invertebrate digestive tracts represent an undescribed clade within the unicellular Opisthokont lineage ichthyosporea (Mesomycetozoea). Protist *162*, 33–57.
51. Dudin, O., Ondracka, A., Grau-Bové, X., Haraldsen, A.A.B., Toyoda, A., Suga, H., Bråte, J., and Ruiz-Trillo, I. (2019). A unicellular relative of animals generates a layer of polarized cells by actomyosin-dependent cellularization. eLife *8* (e49801), https://doi.org/10.7554/eLife.49801.001.
52. Kraus, Y.A. (2006). Morphomechanical programming of morphogenesis in cnidarian embryos. Int. J. Dev. Biol. *50*, 267–275.
53. Komatsu, M. (1976). Wrinkled blastula of the sea-star, *Asterina minor* Hayashi. Dev. Growth Differ. *18*, 435–438.
54. Kraus, Y., Flici, H., Hensel, K., Plickert, G., Leitz, T., and Frank, U. (2014). The embryonic development of the cnidarian *Hydractinia echinata*. Evol. Dev. *16*, 323–338.
55. Sebé-Pedrós, A., de Mendoza, A., Lang, B.F., Degnan, B.M., and Ruiz-Trillo, I. (2011). Unexpected repertoire of metazoan transcription factors in the unicellular holozoan *Capsaspora owczarzaki*. Mol. Biol. Evol. *28*, 1241–1254.
56. Dickinson, D.J., Nelson, W.J., and Weis, W.I. (2012). An epithelial tissue in *Dictyostelium* challenges the traditional origin of metazoan multicellularity. BioEssays *34*, 833–840.
57. Nakanishi, N., Sogabe, S., and Degnan, B.M. (2014). Evolutionary origin of gastrulation: insights from sponge development. BMC Biol. *12*, 26.
58. Li, C., Cheng, M., Zhu, M., and Lyons, T.W. (2018). Heterogeneous and dynamic marine shelf oxygenation and coupled early animal evolution. Emerg. Top. Life Sci. *2*, 279–288.
59. R Development Core Team. (2016). R: A language and environment for statistical computing (R Foundation for Statistical Computing).

STAR★METHODS

KEY RESOURCES TABLE

REAGENT or RESOURCE	SOURCE	IDENTIFIER
Deposited Data		
Caveasphaera fossil specimens	This paper	NIGPAS Collections numbers NIGP 171455 to 171680, 171725 to 171732, Nanjing Institute of Geology, Palaeontology and Stratigraphy, Chinese Academy of Sciences (NIGPAS), Nanjing, China NRM Collections numbers NRM X8334 to X8340 Swedish Museum of Natural History, Stockholm, Sweden
Tomographic datasets and associated computed tomographic models	This paper	Bristol University Research Data Repository https://data.bris.ac.uk/data/
Software and Algorithms		
AVIZO 9.0	Thermo Fisher	https://www.thermofisher.com
VG StudioMax 3.0	Volume Graphics	https://www.volumegraphics.com

LEAD CONTACT AND MATERIALS AVAILABILTY

Further information and requests for resources and reagents should be directed to and will be fulfilled by the Lead Contact Philip Donoghue (phil.donoghue@bristol.ac.uk).

EXPERIMENTAL MODEL AND SUBJECT DETAILS

The specimens described in this study are available at Nanjing Institute of Palaeontology and Stratigraphy Chinese Academy of Sciences (NIGPAS), Nanjing, China under collections numbers NIGP 171455 to 171680, 171725 to 171732 and the Swedish Museum of Natural History, Box 50007, SE-104 05, Stockholm, Sweden under collections numbers NRM X8334 to X8340.

METHOD DETAILS

Specimen recovery

Specimens were recovered from rock samples from the Upper Phosphorites of the Datang and 54 quarries, Weng'an, Guizhou Province, China [21]. The carbonate constituents of the samples were dissolved in ca 8%–10% acetic acid and the phosphatised fossils were recovered from the resulting residues by manual sorting under a binocular microscope. Figured specimens are deposited at Nanjing Institute of Geology and Palaeontology, Chinese Academy of Sciences (NIGPAS). Selected specimens were also examined using a scanning electronic microscope (Leo VP1530) operating at voltage ranging from 5 to 20 KV.

Scanning Electron Microscopy

Selected specimens were also examined using a scanning electronic microscope (Leo VP1530) operating at voltage ranging from 5 to 20 kv, at the Nanjing Institute of Palaeontology and Stratigraphy, Chinese Academy of Sciences, Nanjing, China.

X-Ray and Computed Tomography

Tomographic scanning was carried out at the X02DA (TOMCAT) beamline of Swiss Light Source (Paul Scherrer Institute, Switzerland) and at the micro-CT lab of NIGPAS, using srXTM [19] and high-resolution X-ray microtomography [20]. The tomographic data were analyzed using AVIZO and VG StudioMax (3.0) software. A three-dimensional model was reconstructed for each specimen and the body volume was calculated in Avizo or VG StudioMax from the segmented model. As the specimens are not perfect spheres, the diameter of *Caveasphaera* was calculated as the average of three (x, y, z) body measurements. 233 specimens were scanned and, 70 of them show well-preserved cellular structures (Data S1). The volume data for all of the 233 specimens (2.5Tb) are available at https://data.bris.ac.uk/data/dataset/7eku32izrw5s2nrno2m0oxtj1 Volume data for 100 unbroken specimens were segmented to measure the body diameter, number of isolated cell clusters and sum volume of cell mass. Based on the segmented volume data of the specimens showing the best cell preservation with clear membranes, individual volumes of 137 internal cells (within the main body) of 27 specimens across different developmental stages were measured, and 48 surface cells (in contact with the surface of the main body) of 8 specimens with different sizes were measured. Cell volumes were calculated in Avizo using the material statistics function.

QUANTIFICATION AND STATISTICAL ANALYSIS

Graphs and statistical analyses were performed using R [59].

DATA AND CODE AVAILABILITY

The tomographic datasets and associated computed tomographic models are available from Bristol University Research Data Repository https://data.bris.ac.uk/data/dataset/7eku32izrw5s2nrno2m0oxtj1